Impact of current LHC results on Selected Higgs Scenarios

Jack Gunion
U.C. Davis

KITP Snowmass Workshop, May 29, 2013

Higgs couplings Collaborators: Belanger, Beranger, Ellwanger, Kraml

1. *"Status of invisible Higgs decays"* G. Belanger, B. Dumont, U. Ellwanger, J. F. Gunion and S. Kraml. arXiv:1302.5694 [hep-ph]
2. *"Higgs Couplings at the End of 2012"* G. Belanger, B. Dumont, U. Ellwanger, J. F. Gunion and S. Kraml. arXiv:1212.5244 [hep-ph]
3. *"Global fit to Higgs signal strengths and couplings and selected model implications"* G. Belanger, B. Dumont, U. Ellwanger, J. F. Gunion and S. Kraml. In preparation

NMSSM Collaborators: G. Belanger, U. Ellwanger, Y. Jiang, S. Kraml, J. Schwarz

1. *"Higgs Bosons at 98 and 125 GeV at LEP and the LHC"* G. Belanger, U. Ellwanger, J. F. Gunion, Y. Jiang, S. Kraml and J. H. Schwarz. arXiv:1210.1976 [hep-ph]
2. *"Two Higgs Bosons at the Tevatron and the LHC?"* G. Belanger, U. Ellwanger, J. F. Gunion, Y. Jiang and S. Kraml. arXiv:1208.4952 [hep-ph]

3. *"Diagnosing Degenerate Higgs Bosons at 125 GeV"* J. F. Gunion, Y. Jiang and S. Kraml. arXiv:1208.1817 [hep-ph]
4. *"Could two NMSSM Higgs bosons be present near 125 GeV?"* J. F. Gunion, Y. Jiang and S. Kraml. arXiv:1207.1545 [hep-ph]
5. *"The Constrained NMSSM and Higgs near 125 GeV"* J. F. Gunion, Y. Jiang and S. Kraml. arXiv:1201.0982 [hep-ph] Phys. Lett. B **710**, 454 (2012)

2HDM Collaborators: Alexandra Drozd, Bohdan Grzadkowski, Yun Jiang

1. *"Two-Higgs-Doublet Models and Enhanced Rates for a 125 GeV Higgs"* A. Drozd, B. Grzadkowski, J. F. Gunion and Y. Jiang. arXiv:1211.3580 [hep-ph]
2. *"Fitting the LHC Higgs signal in Two-Higgs-Doublet Models"* B. Dumont, J. F. Gunion, Y. Jiang and S. Kraml. In preparation

Quantifying the observed signal

- **Production modes: ggF, ttH, VBF, VH**
- **Decay modes: $\gamma\gamma$, $ZZ^{(*)}$, $WW^{(*)}$, $b\bar{b}$ and $\tau\tau$**

- **If we have custodial symmetry and if $b\bar{b}$ and $\tau\tau$ rescale by a common factor as in many models, then we are left with two independent production modes (VBF+VH) and (ggF+ttH), and three independent final states $\gamma\gamma$, $VV^{(*)}$ and $b\bar{b} = \tau\tau$.**
- **In recent publications by the ATLAS and CMS collaborations, likelihoods are given in the (VBF+VH) and (ggF+ttH) plane for relative signal strengths μ_i in the specific final states $\gamma\gamma$, $ZZ^{(*)}$, $WW^{(*)}$, $b\bar{b}$, $\tau\tau$.**

  Using the the ellipses provided, we are able to include the rather important correlations due to mutually common errors of the (VBF+VH) and (ggF+ttH) production processes.
- **We combine the information provided by ATLAS, CMS and the Tevatron on the likelihoods as function of the six independent signal strengths μ_i defined above.**

  An illustration of the kind of plots we combine are those for ATLAS as given below —though not perfect ellipses, we fit them as ellipses and then combine with other experiments.

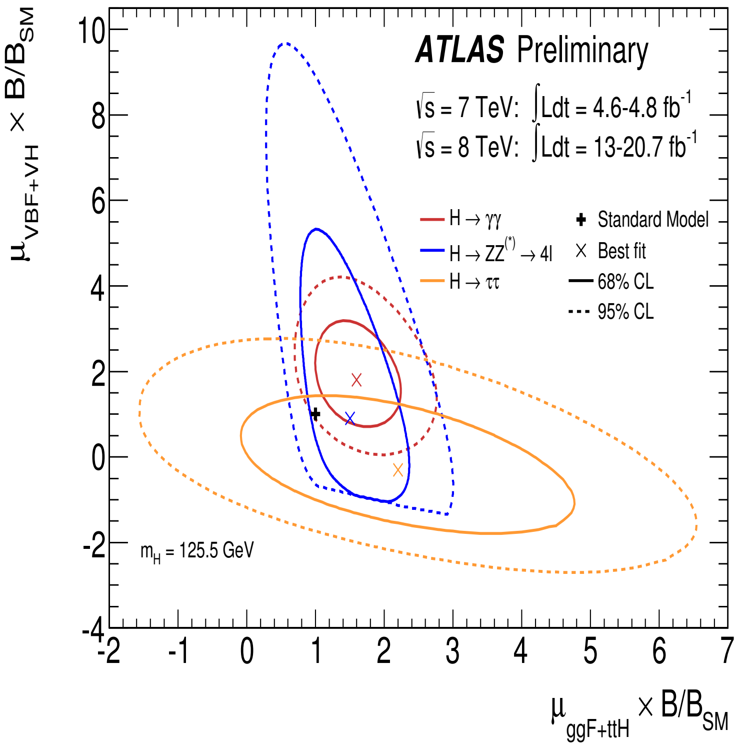

Figure 1: ATLAS results, including 4ℓ, $\gamma\gamma$ and $\tau\tau$.

- **The results appear in the following figure.**

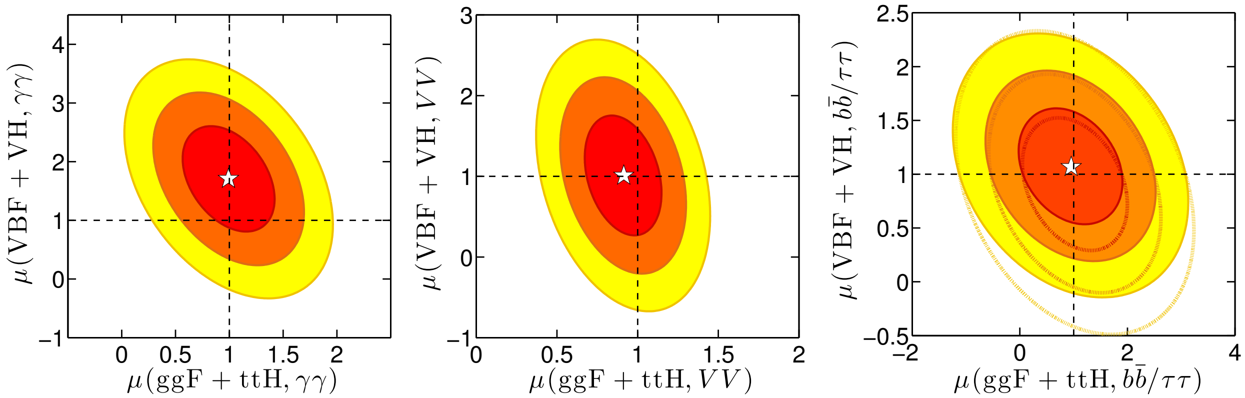

Figure 2: Combined signal strength ellipses for the $\gamma\gamma$, $VV = ZZ, WW$ and $DD = b\bar{b}, \tau\tau$ channels. The filled red, orange and yellow ellipses show the 68%, 95% and 99.7% CL regions, respectively, derived by combining the ATLAS, CMS and Tevatron results. The line contours in the right-most plot show how these ellipses change when neglecting the Tevatron results. The white stars mark the best-fit points.

Certainly, the SM is doing quite well.

- To formulate this statement more precisely we can look at the impact on generalized SM-like couplings:

$$\begin{aligned}\mathcal{L} &= g\Big[C_V\left(m_W W_\mu W^\mu + \frac{m_Z}{\cos\theta_W} Z_\mu Z^\mu\right) \\ &\quad - C_U \frac{m_t}{2m_W}\bar{t}t - C_D\frac{m_b}{2m_W}\bar{b}b - C_D\frac{m_\tau}{2m_W}\bar{\tau}\tau\Big] H\,. \end{aligned} \tag{1}$$

where $C_U = C_D = C_V = 1$ in the SM.

- In addition to these "tree-level" couplings there are also loop-induced couplings $gg \to H$ and $\gamma\gamma \to H$, the former dominated by the top-quark loop and the latter dominated by the W loop with a smaller and opposite contribution from a top-quark loop.

  Given values for C_U, C_D and C_V the contributions of SM particles to the gg and $\gamma\gamma$ couplings, denoted $\overline{C}_g$ and $\overline{C}_\gamma$ respectively, can be computed.

  In some of the fits below, we will also allow for additional new physics contributions to C_g and C_γ by writing $C_g = \overline{C}_g + \Delta C_g$ and $C_\gamma = \overline{C}_\gamma + \Delta C_\gamma$.

- $\boxed{C_U = C_D = C_V = 1 \text{ with free } \Delta C_\gamma \text{ and } \Delta C_g}$

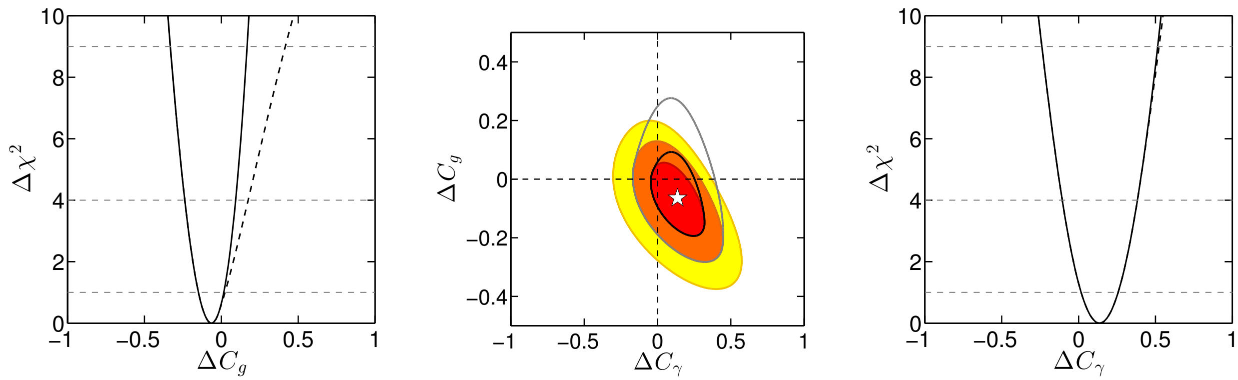

Figure 3: In the 1D plots, the solid (dashed) lines are for the case that invisible/unseen decays are absent (allowed). Red, orange and yellow areas are the 68%, 95% and 99.7% CL regions, respectively, assuming invisible decays are absent. The black and grey ellipses show the 68% and 95% CL contours when allowing for invisible decays.

- Since one finds that $C_U < 0$ is now disfavored and the sign of C_D is irrelevant, we confine ourselves subsequently to $C_U, C_D > 0$. In Fig. 4 we show $\Delta\chi^2$ distributions in 2D planes confined to this range.

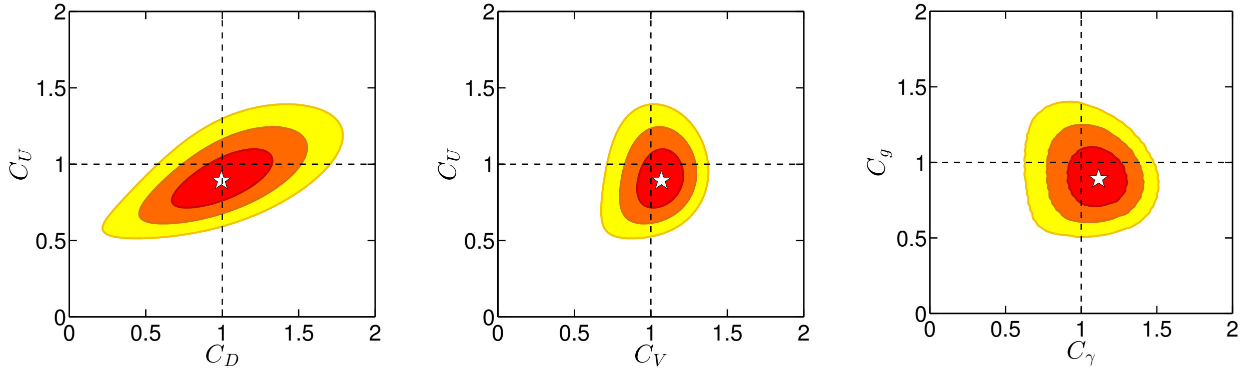

Figure 4: Fit of $C_U > 0$, $C_D > 0$ and C_V for $\Delta C_g = \Delta C_\gamma = 0$. The red, orange and yellow areas are the 68%, 95% and 99.7% CL regions, respectively, assuming invisible decays are absent. The white star marks the best-fit point.

- The best fit is obtained for $C_U = 0.89$, $C_D = 0.99$, $C_V = 1.07$, $C_\gamma = 1.11$, $C_g = 0.89$ (and, in fact, $\mathcal{B}_{\rm inv} \equiv \mathcal{B}(H \to {\rm invisible}) = 0$).

- Note that if $C_V > 1$ were confirmed, this would imply that the observed Higgs boson must have a triplet (or higher representation) component.

- Currently the coupling fits are, however, perfectly consistent with SM values. Indeed, with a $\chi^2_{\rm min} = 17.6$ as compared to $\chi^2 = 18.97$ for the SM, allowing for deviations from the SM does not significantly improve the fit.

- $\boxed{C_U \geq 0,\ C_D \geq 0,\ C_V \leq 1}$

If the Higgs sector consists of doublets+singlets only, then $C_V \leq 1$. Results for this case are shown in Fig. 5.

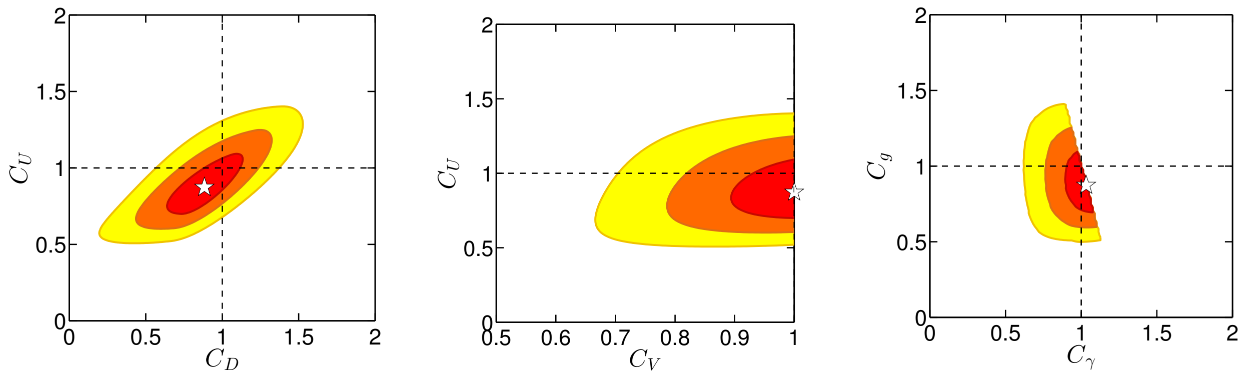

Figure 5: **Fit of C_U, C_D, C_V for $\Delta C_g = \Delta C_\gamma = 0$, as in Fig. 4 but for $C_V \leq 1$.**

Given the slight preference for $C_V > 1$ in the previous free-C_V plots, it is no surprise that $C_V = 1$ provides the best fit along with $C_U = C_g = 0.87$, $C_D = 0.88$ and $C_\gamma = 1.03$. Of course, the SM is again well within the 68% CL zone.

- $\boxed{C_U \geq 0,\ C_D \geq 0,\ C_V \leq 1,\ \text{free } \Delta C_g, \Delta C_\gamma}$

The general case of free parameters C_U, C_D, C_V, ΔC_g and ΔC_γ is illustrated in Fig. 6, where we show the 1D $\Delta\chi^2$ distributions for these five parameters (each time profiling over the other four parameters).

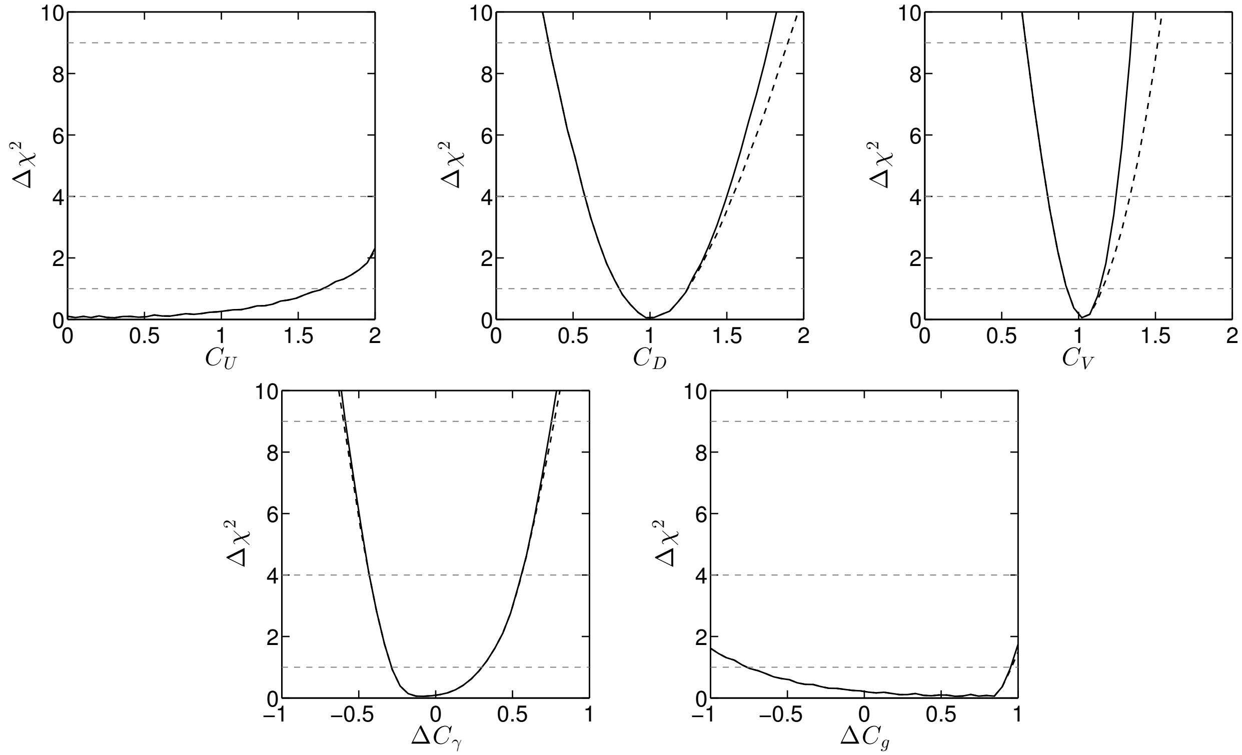

Figure 6: **Five (six) parameter fit of C_U, C_D, C_V, ΔC_g and ΔC_γ; the solid (dashed) curves are those obtained when invisible / unseen decay modes are not allowed (allowed) for.**

- **As before, the solid (dashed) lines indicate results not allowing for (allowing for) invisible/unseen decay modes of the Higgs.**
- **Allowing for invisible/unseen decay modes again relaxes the $\Delta\chi^2$ behavior only modestly.**
- **The best fit point always corresponds to $\mathcal{B}_{\rm inv} = 0$.**

- **Invisible Decays**

An overview of the current status of invisible decays is given in Fig. 7, which shows the behavior of $\Delta\chi^2$ as a function of $\mathcal{B}_{\rm inv}$ for various different cases of interest:
a) SM Higgs with allowance for invisible decays — one finds $\mathcal{B}_{\rm inv} < 0.08$;
b) $C_U = C_D = C_V = 1$ but $\Delta C_\gamma, \Delta C_g$ allowed for — $\mathcal{B}_{\rm inv} < 0.09$;
c) C_U, C_D, C_V free, $\Delta C_\gamma = \Delta C_g = 0$, — $\mathcal{B}_{\rm inv} < 0.15$;
d) C_U, C_D free, $C_V \leq 1$, $\Delta C_\gamma = \Delta C_g = 0$ — $\mathcal{B}_{\rm inv} < 0.08$;
e) $C_U, C_D, C_V, \Delta C_g, \Delta C_\gamma$ free — $\mathcal{B}_{\rm inv} < 0.15$.
(All $\mathcal{B}_{\rm inv}$ limits are at 1σ or 68% CL.)

Thus, while $\mathcal{B}_{\rm inv}$ is certainly significantly limited by the current data set, there remains ample room for invisible / unseen decays. At 2σ or 95% CL, $\mathcal{B}_{\rm inv}$ as large as ~ 0.37 is possible.

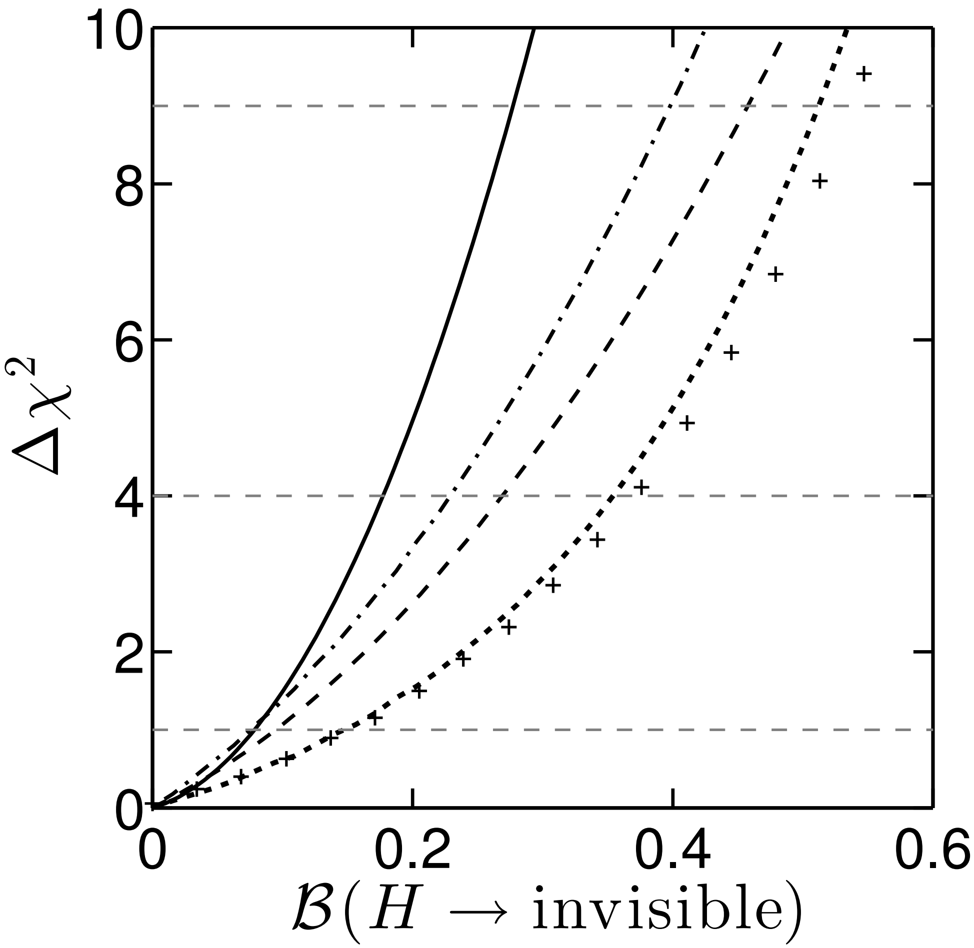

Figure 7: $\Delta\chi^2$ distributions for the branching ratio of invisible Higgs decays for various cases. **Solid:** SM+invisible. **Dot-dashed:** varying C_U, C_D, $C_V \leq 1$ for $\Delta C_g = \Delta C_\gamma = 0$. **Dashed:** varying ΔC_g and ΔC_γ for $C_U = C_D = C_V = 1$. **Dotted:** varying C_U, C_D, C_V for $\Delta C_g = \Delta C_\gamma = 0$. **Crosses:** varying C_U, C_D, C_V, ΔC_g and ΔC_γ.

- **Total Width**

The global fit we perform here also makes it possible to constrain the Higgs boson's total decay width, $\Gamma_{\rm tot}$, a quantity which is not directly measurable at the LHC.

For SM + invisible decays, we find $\Gamma_{\rm tot}/\Gamma_{\rm tot}^{\rm SM} < 1.09$ (1.22) at 68% (95%) CL.

Figure 8 shows the $\Delta\chi^2$ as function of $\Gamma_{\rm tot}/\Gamma_{\rm tot}^{\rm SM}$ for the fits of C_U, C_D, $C_V \leq 1$; C_U, C_D, C_V free; and C_U, C_D, C_V, ΔC_g, ΔC_γ.

The case of ΔC_g, ΔC_γ with $C_U = C_D = C_V = 1$ is not shown; without invisible decays we find $\Gamma_{\rm tot}/\Gamma_{\rm tot}^{\rm SM} = [0.97, 1.12]$ ($[0.95, 1.41]$) at 68% (95%) CL in this case.

Allowing for invisible decays this changes to $\Gamma_{\rm tot}/\Gamma_{\rm tot}^{\rm SM} = [0.70, 1.38]$, ($[0.45, 1.82]$), *i.e.* it is very close to the line for C_U, C_D, $C_V \leq 1$ in the right plot of Fig. 8.

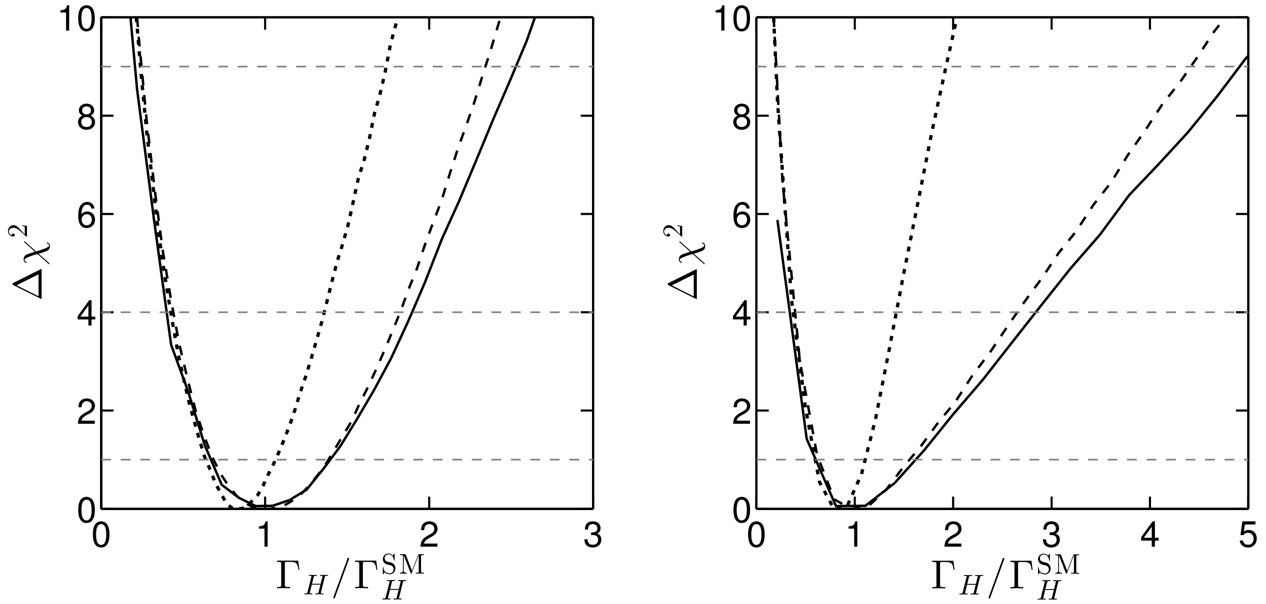

Figure 8: $\boldsymbol{\Delta\chi^2}$ **distributions for** $\boldsymbol{\Gamma_{\rm tot}/\Gamma_{\rm tot}^{\rm SM}}$**, on the left without invisible decays, on the right including** $\boldsymbol{\mathcal{B}_{\rm inv}}$ **as a free parameter in the fit. The lines are for:** $\boldsymbol{C_U>0}$**,** $\boldsymbol{C_D>0}$**,** $\boldsymbol{C_V\leq 1}$ **(dotted),** $\boldsymbol{C_U>0}$**,** $\boldsymbol{C_D>0}$**,** $\boldsymbol{C_V}$ **(dashed),** $\boldsymbol{C_U>0}$**,** $\boldsymbol{C_D>0}$**,** $\boldsymbol{C_V}$**,** $\boldsymbol{\Delta C_g}$**,** $\boldsymbol{\Delta C_\gamma}$ **(solid).**

Application of fits to specific models

- So far our fits have been largely model-independent, relying only on assuming the Lagrangian structure of the SM.

  Let us now apply our fits to some concrete examples of specific models, giving relations between some of the coupling factors C_I.

- **Triplet Higgs model**

- We consider the Georgi-Machacek model which combines a single Higgs doublet field with $Y = 0$ and $Y = \pm 1$ triplet fields in such a way that custodial symmetry is preserved at tree level. The phenomenology of this model was developed in detail by Gunion and Vega.

- In this model, the neutral doublet and triplet fields acquire vacuum expectation values given by: $\langle \phi^0 \rangle = a/\sqrt{2}$ and $\langle \chi^0 \rangle = \langle \xi^0 \rangle = b$, respectively.

  It is the presence of the two triplet fields and their neutral members having the same vev, b, that guarantees $\rho = 1$ at tree level.

- The value of $v^2 \equiv a^2 + 8b^2 = (246~\mathrm{GeV})^2$ is determined by the W, Z masses.

  However, the relative magnitude of a and b is a parameter of the model. The relative mixture is defined by the doublet-triplet mixing angle θ_H with cosine and sine given by $c_H = \frac{a}{\sqrt{a^2+8b^2}}$ and $s_H \equiv \sqrt{\frac{8b^2}{a^2+8b^2}}$.

  The angle θ_H is reminiscent of the β angle of a 2HDM.

- In this model, it is most natural to choose a Higgs sector potential that preserves the custodial symmetry.
- Then, the only Higgs state that can be related to the $125.5~\mathrm{GeV}$ signal is the H_1^0 with some mixture of $H_1^{0\prime}$ possible.

  Their mass-squared matrix will be diagonalized by a rotation matrix specified by an angle for which we use the 2HDM-like notation, α.
- The reduced couplings of H_1^0 and $H_1^{0\prime}$ are given by

$$C_F(H_1^0) = \frac{1}{c_H}, \quad C_V(H_1^0) = c_H, \quad C_F(H_1^{0\prime}) = 0, \quad C_V(H_1^{0\prime}) = \frac{2\sqrt{2}}{\sqrt{3}} s_H\,, \tag{2}$$

  where all fermionic coupling scale with the common factor C_F.
- In terms of α, we can write the Higgs boson mass eigenstates as

$$H = \cos\alpha H_1^0 + \sin\alpha H_1^{0\prime}, \quad H' = -\sin\alpha H_1^0 + \cos\alpha H_1^{0\prime}. \tag{3}$$

  When studying the $125.5~\mathrm{GeV}$ state, its SM-like nature suggests it should be identified with the H since for $\alpha, s_H \to 0$ the H is identical in properties to the SM Higgs.

  The couplings of the H relative to the SM are:

$$C_F = \frac{\cos\alpha}{c_H}, \qquad C_V = c_H \cos\alpha + \frac{2\sqrt{2}}{\sqrt{3}} s_H \sin\alpha\,. \tag{4}$$

  Note that if s_H is sizable, then C_V will be enhanced relative the SM value of 1 and the fermionic couplings will also be enhanced.

- So, the interesting question is what does the LHC data allow for θ_H and α.
  The result is shown in Fig. 9, on the left in the θ_H versus α plane and on the right in the C_V versus C_U plane.

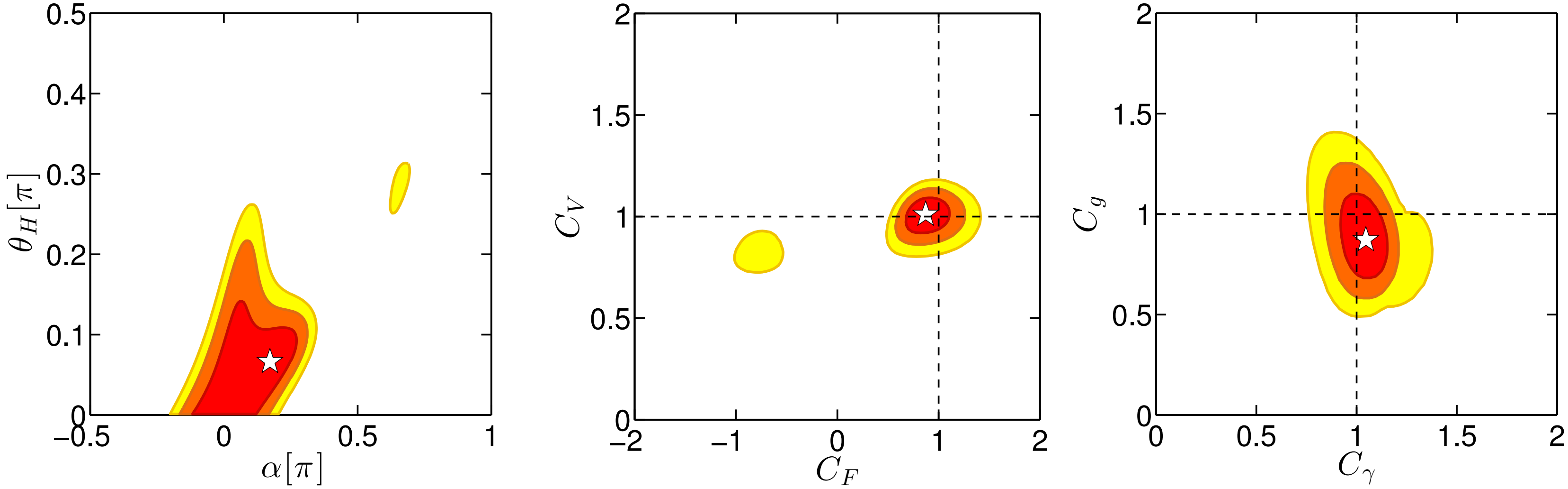

Figure 9: Fit for Georgi–Machacek triplet model assuming that $H = \cos\alpha H_1^0 + \sin\alpha H_1^{0\prime}$ is the observed state at 125.5 GeV.

- With regard to the H', whose couplings relative to the SM are:

$$C'_F = -\frac{\sin\alpha}{c_H}, \qquad C'_V = \frac{2\sqrt{2}}{\sqrt{3}} s_H \cos\alpha - c_H \sin\alpha\,. \tag{5}$$

  We note that $\alpha \sim 0$, $s_H \sim 0$ and $c_H \sim 1$ imply that the H' couplings to both fermions and vector bosons are small. (Plots are under development.)
  Thus, unlike the H of the 2HDM which can have reasonable $f\overline{f}$ (but not VV) couplings

and thus reasonable production rate, ggF and VBF H' production rates will both be small. However, looking at the mass-squared matrix for small s_H, one finds that the H' (primarily $H_1^{0\,\prime}$ for the choice we have made with H_1^0 at $125~\mathrm{GeV}$) is likely to be quite light and that may allow some chance for discovery —- for example, $H \to H'H'$ decays are possible (but can't be too large without destroying the SM rates for the H).

- **The 2HDM**

  In the figures to follow,

- grey points satisfy all constraints related to B-physics, Precision Electroweak (STU), and stability, unitarity and perturbativity (SUP), but fail one or more of the LHC Higgs results at the 95% CL.

  All the colored points satisfy B,STU,SUP and one or more LHC Higgs measurements.
- cyan points satisfy 95% CL limits on $4l$ rates at masses above $130~\mathrm{GeV}$ (before rescaling for the narrow width), but not necessarily limits in other channels.
- gold points satisfy $bb, \tau\tau$ 95% CL limits for the $125.5~\mathrm{GeV}$ state, but not necessarily limits in other channels.
- blue points satisfy WW, ZZ 95% CL limits, but not necessarily limits in other channels.
- green points satisfy $\gamma\gamma$ 95% CL limits, but not necessarily limits in other channels.
- light red points satisfy all LHC Higgs results (before width rescaling).
- dark red points satisfy all LHC Higgs results even after rescaling the width.

Points are plotted in the above order, so earlier colors are sometimes overwritten.

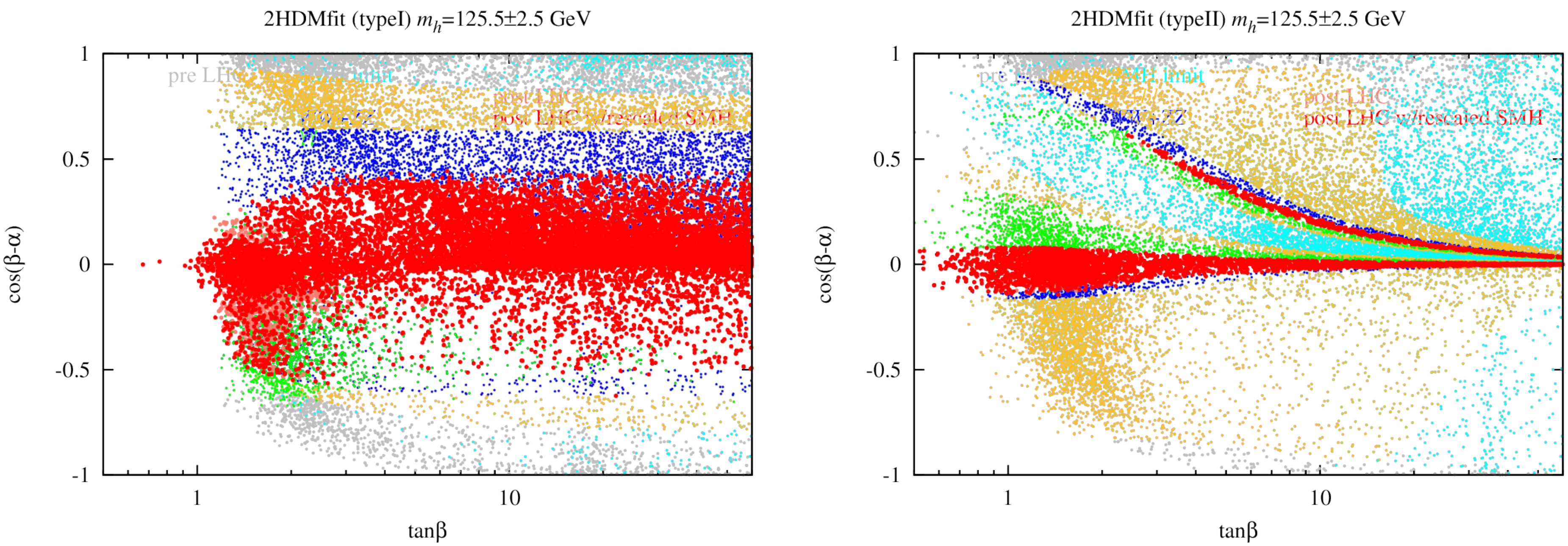

Figure 10: **Constraints on the 2HDM models of Type I and II in the $\cos(\beta-\alpha)$ versus $\tan\beta$ plane for $m_h \sim 125.5$ GeV (upper row) and in the $\sin(\beta-\alpha)$ versus $\tan\beta$ plane for $m_H \sim 125.5$ GeV (lower row).**

- **Given that the SM limit is $\cos(\beta-\alpha) \to 0$, we see that much greater precision is needed for Type I, whereas for Type II there is a main branch that is very SM-like, but also an alternative branch that is quite different. What will the future LHC run say?**
- **Also of interest for the $m_h \sim 125.5$ GeV case are plots of heavier Higgs masses as functions of $\cos(\beta-\alpha)$.**

  These are given in Fig. 11, where we see clearly that once m_H, m_A are above about 800 GeV we are deep into the small $|\cos(\beta-\alpha)|$ decoupling region, whereas for masses below ~ 800 GeV there is considerable spread in the allowed $|\cos(\beta-\alpha)|$ values.

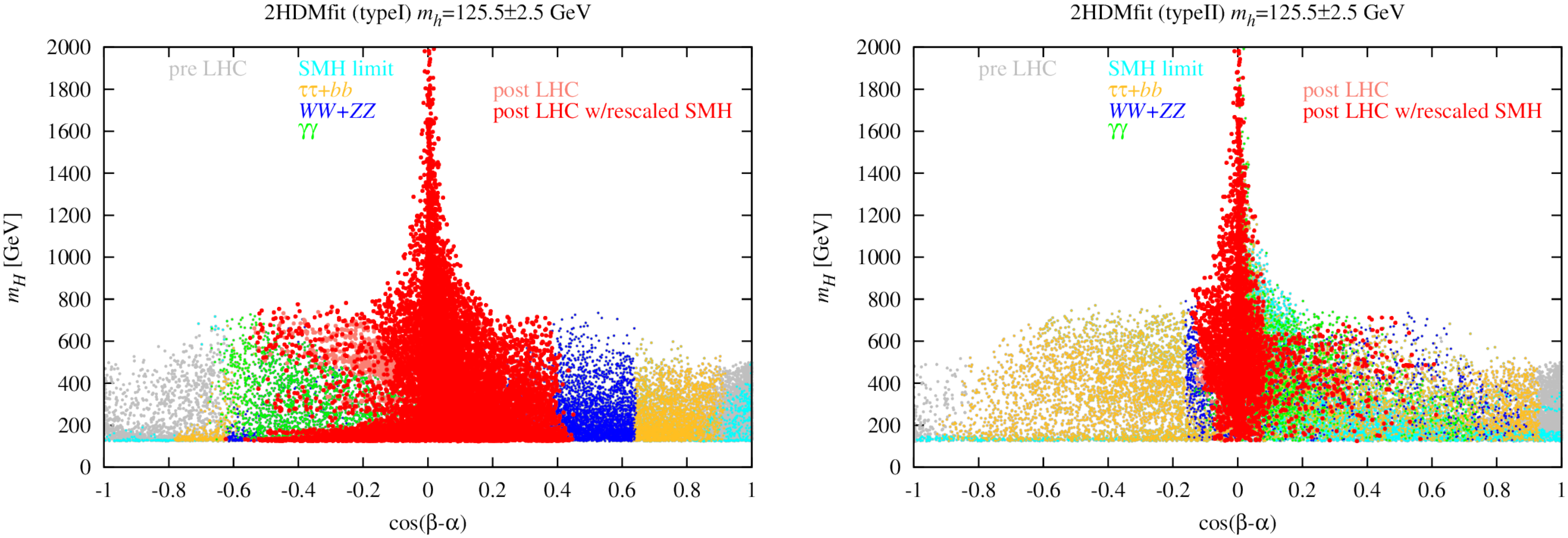

Figure 11: Points in the m_H vs. $\cos(\beta-\alpha)$ vs. $\cos(\beta-\alpha)$ plane following the notation of Fig. 10. Results in the $m_{H^\pm}, m_A$ vs. $\cos(\beta-\alpha)$ planes are very like those for m_H vs. $\cos(\beta-\alpha)$.

- Of course, an important question is whether the Higgs bosons other than the one with mass of order 125 GeV will be observable or not. This can be revealed by using the well known μ ratios discussed earlier, but now for the heavier Higgs, for a given rate relative to the corresponding rate for the SM Higgs boson. The ZZ ratios for the case of $m_h \sim 125.5~\mathrm{GeV}$ appear in Fig. 12.

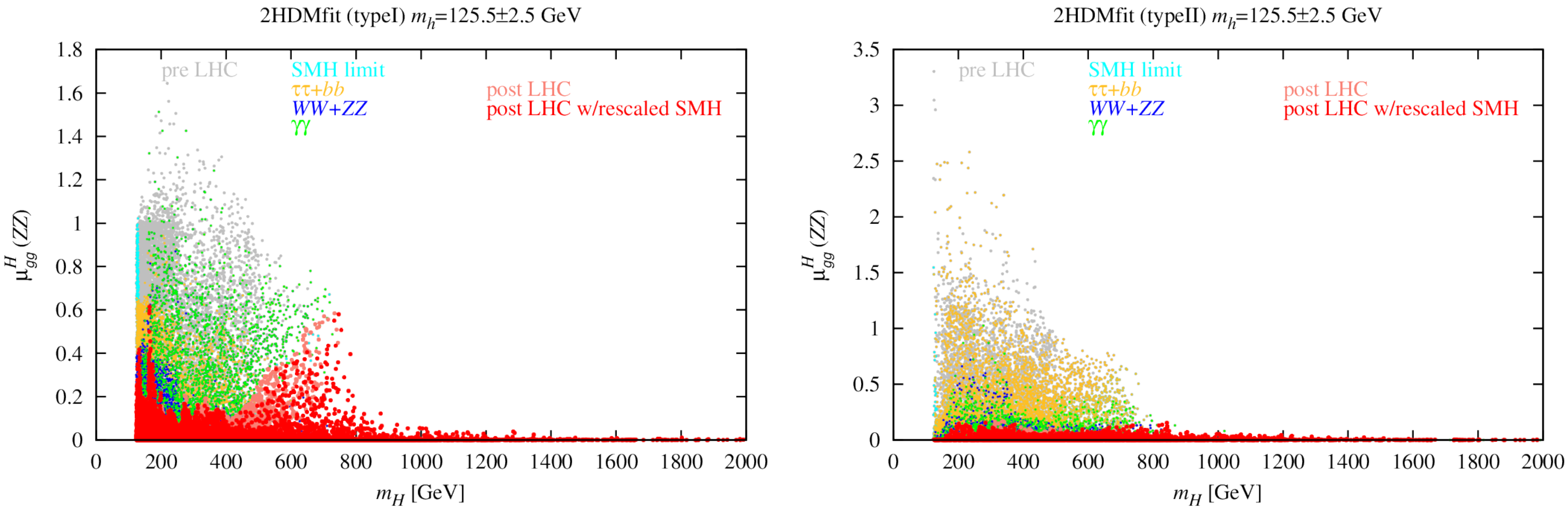

Figure 12: $\mu^H_{gg}(ZZ)$ ratio for $H \to ZZ$ as a function of m_H when $m_h = 125.5$ GeV.

There we see that the $gg \to H \to ZZ$ rate can be significant relative to the SM in the case of Type I, but Type II rates are mostly modest in size.

- Of course, it should be noted that the width of the H can be very much smaller than for the h_{SM} at the same mass. This will help discovery, but study is needed to quantify.
- Viability of an H signal in other channels also deserves study.

  Natural possibilities include $\gamma\gamma$ and $\tau\tau$.
- For the $\gamma\gamma$ final state we find:

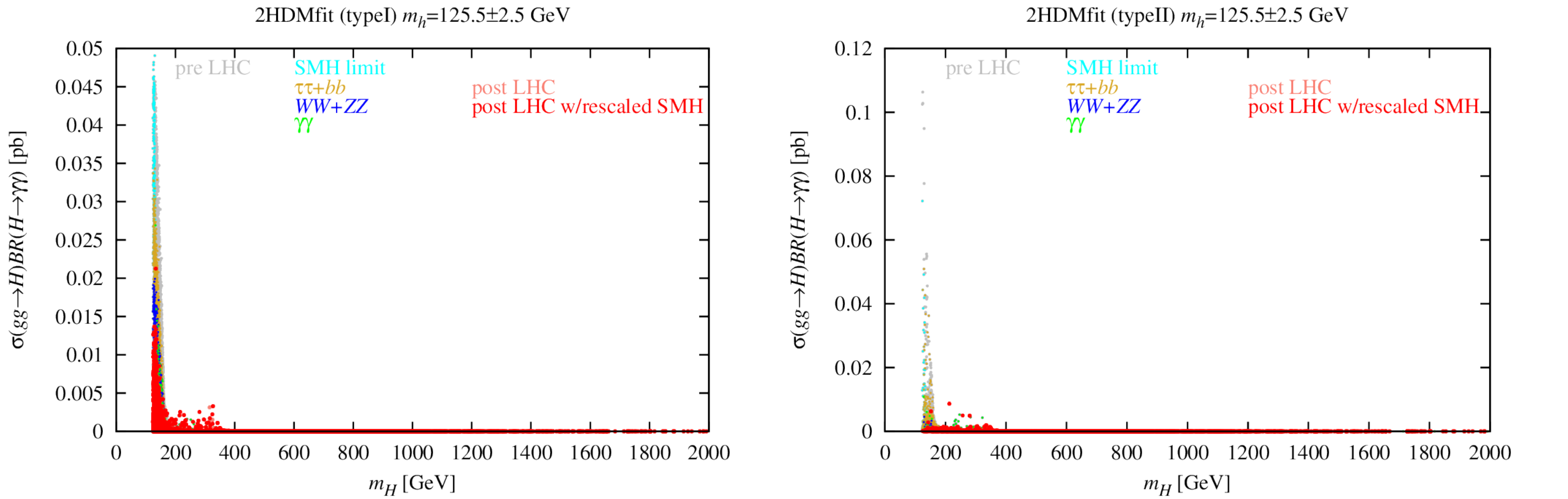

Figure 13: For $m_h \sim 125.5~\mathrm{GeV}$, we plot $\sigma_{gg}^{H} \times \mathcal{B}(H \to \gamma\gamma)$ as a function of m_H. Backgrounds at high m_H need to be determined, but mass resolution should remain good.

- Also of potential interest are the rates for $gg \to H, A \to \tau\tau$.

- **Another possible channel is $H \to hh$. This can have a large branching ratio.**

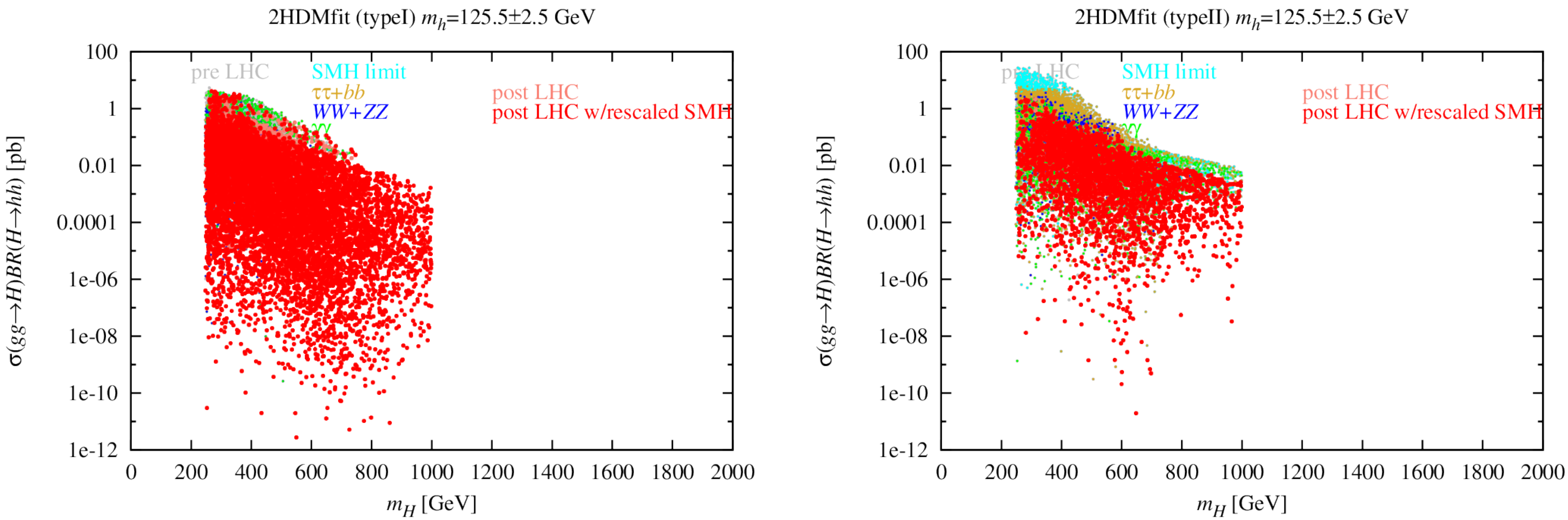

Figure 14: For $m_h \sim 125.5\ \mathrm{GeV}$, we plot $\sigma_{gg}^{H} \times \mathcal{B}(H \to hh)$. Plots stop at $m_h = 1\ \mathrm{TeV}$ since 'official' cross sections stop there.

- **General Lesson**

  Even though we have pretty accurate measurements for the $125.5\ \mathrm{GeV}$ state properties, we have a long way to go before we can be certain that the other Higgs bosons of the 2HDM are not present at 'reasonable' masses.

Conclusions

- It seems likely that the Higgs responsible for EWSB has emerged.
- At the moment, there is no sign of other Higgs-like signals except hints at $\sim 140~\mathrm{GeV}$ and the old LEP excess at $98~\mathrm{GeV}$.
- Survival of enhanced signals for the $125~\mathrm{GeV}$ state would be one of the most exciting outcomes of the current LHC run and would guarantee years of theoretical and experimental exploration of BSM models with elementary scalars.
- $>$SM signals would appear to guarantee the importance of a linear collider or LEP3 or muon collider in order to understand fully the responsible BSM physics.
- Although current data is converging to a SM-like Higgs, there is still room for additional Higgs bosons in important model classes.

  Thus, we must push hard to improve errors on the nature of the $125~\mathrm{GeV}$ state since even small deviations could be a first sign of such additional states.